Intensity Distribution of the X-Ray Source for the AXAF VETA-I Mirror Test

Ping Zhao, Edwin M. Kellogg, Daniel A. Schwartz, and Yibo Shao

Harvard-Smithsonian Center for Astrophysics
60 Garden Street, Cambridge, MA 02138

M. Ann Fulton

ES-65, Marshall Space Flight Center, AL 35812

ABSTRACT

The X-ray generator for the AXAF VETA-I mirror test is an electron impact X-ray source with various anode materials. The source sizes of different anodes and their intensity distributions were measured with a pinhole camera before the VETA-I test. The pinhole camera consists of a 30 μm diameter pinhole for imaging the source and a Microchannel Plate Imaging Detector with 25 μm FWHM spatial resolution for detecting and recording the image. The camera has a magnification factor of 8.79, which enables measuring the detailed spatial structure of the source. The spot size, the intensity distribution, and the flux level of each source were measured with different operating parameters.

During the VETA-I test, microscope pictures were taken for each used anode immediately after it was brought out of the source chamber. The source sizes and the intensity distribution structures are clearly shown in the pictures. They are compared and agree with the results from the pinhole camera measurements.

This paper presents the results of the above measurements. The results show that under operating conditions characteristic of the VETA-I test, all the source sizes have a FWHM of less than 0.45 mm. For a source of this size at 528 meters away, the angular size to VETA is less than 0.17 arcsec which is small compared to the on ground VETA angular resolution (0.5 arcsec, required and 0.22 arcsec, measured). Even so, the results show the intensity distributions of the sources have complicated structures. These results were crucial for the VETA data analysis and for obtaining the on ground and predicted in orbit VETA Point Response Function.

1. INTRODUCTION

The Advanced X-ray Astrophysical Facility (AXAF) is NASA's third Great Space Observatory, scheduled to be launched in the late 1990s.[1] The main element of AXAF is its X-ray telescope which consists of four nested Wolter Type-I mirror pairs. The Verification Engineering Test Article-I (VETA-I), made of Zerodur with a diameter of 1.2 meters, is the uncoated outmost pair.[2] Its mirror figures and surface quality were measured using an electron impact X-ray source at the X-ray Calibration Facility (XRCF) of the Marshall Space Flight Center (MSFC) from August to October of 1991. X-rays generated in the source chamber traveled 528 meters inside a X-ray Guide Tube before reaching the VETA, and were then focused in the focal plane 10 meters behind the VETA. Four types of measurement were made as listed below with their required precisions:

- Full Width Half Maximum (FWHM, expected less than 0.5 arcsec). $\pm$ 0.05 arcsec.
- Encircled Energy. $\pm$ 2%.
- Effective Area. $\pm$ 5%.
- Ring Focus.

Ideally, a point source with a pure monochromatic line for each energy should be used. But the pure

monochromatic X-ray source does not exist and it is also impossible to construct a point source within a finite distance. Therefore we had to measure the X-ray source spatial and spectral distribution as they were generated in the source chamber. This paper deals with the source spatial distribution. The spectral distribution is discussed elsewhere in this Volume.[3]

The source size and intensity distribution measurement was made at XRCF in June of 1991. The following sections discuss the techniques we used for the measurement, the method we used to analyze the data, and the results. Section 2 briefly describes the X-ray generator of XRCF used for the VETA test. Section 3 explains the pinhole camera setup and the measurement. Section 4 shows the images taken by the pinhole camera and discuss the data analysis process. Section 5 presents the source anode pictures taken during the VETA-I test. Section 6 gives the final results.

2. VETA-I X-RAY GENERATOR

The X-ray Generator Assembly (XGA) at XRCF is housed in the source chamber building and interfaces to the Guide Tube through a 6 inch vacuum gate valve. The other end of the 500 meter Guide Tube is connected with the giant VETA test vacuum chamber in the control building. Figure 1 is a schematic diagram of the XGA. From right to left there are: An alignment telescope port connected to the end of the Guide Tube; then there are bellows and the 6 inch Gate valve. Next to it is the source/filterwheel chamber which houses the filter wheel holding up to nine X-ray filters of different material. Rotating a big feedthrough nob on the top of the chamber enables us to change the filters with in two seconds and without breaking the vacuum. At the end there is the X-ray Generator Head, which houses the X-ray source that produces X-rays by electron bombardment of various anode materials. There is (not shown in the figure) a 2.75 inch gate valve and bellows in between the filterwheel chamber and the Generator Head. The whole XGA is mounted on a Newport optical table. Figure 2 is a simplified view of the X-ray source, which basicly consists of a tungsten filement cathode and a target anode made of various materials. Each anode has a conical shape surface with an angle of 30 degrees from horizontal and 10.7 mm diameter at the bottom. The

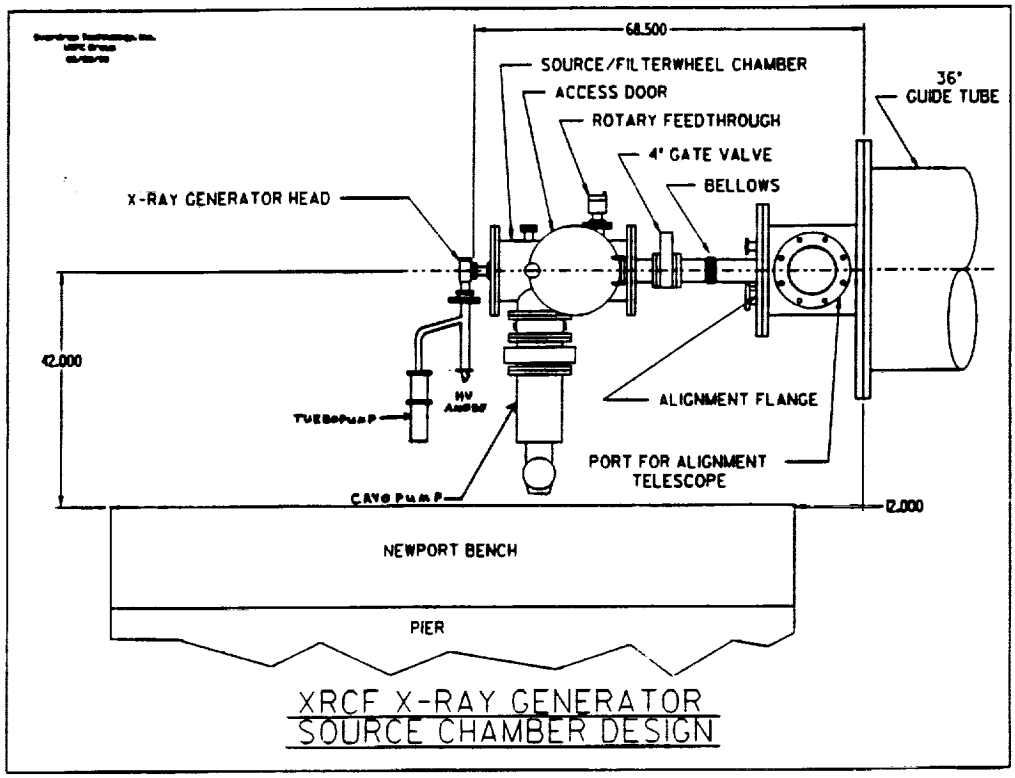

Figure 1: XRCF X-ray Generator Assembly.

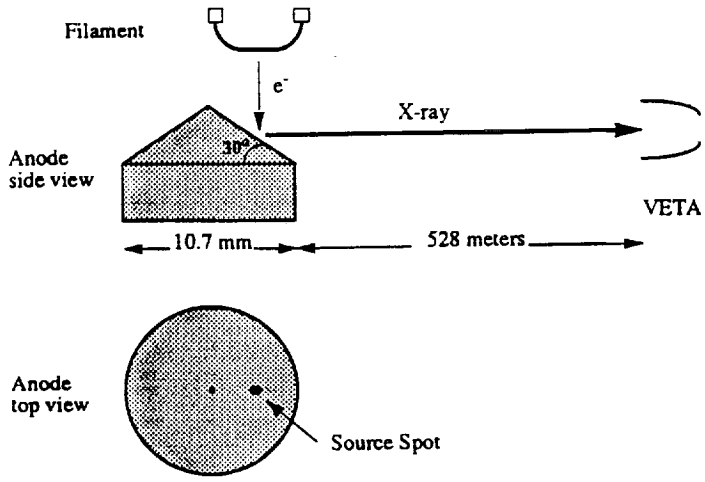

Figure 2: XRCF X-ray Source for the VETA Test.

electron beam, emitted from a heated 0.9 mm diameter tungsten filement located 10 mm above the anode, is accelerated and focused (with a bias focus cap) to a small spot on the target anode. The X-rays produced as a result of the electron - target interaction are projected through a X-ray filter then down the Guide Tube to the experiment. The X-ray source size is limited by the dimensions of the electron impact area rather than by an aperture. The output of the X-ray source is principally characteristic of K and L lines from the anode material superimposed on a bremsstrahlung continuum. The X-ray energy and flux may therefore be controlled by proper selection of target material and electron beam energy, which is controlled by the anode voltage. Proper selected filters are used to suppress the bremsstrahlung continuum and low energy photons. Generally, filters are made of the same material as the target since the characteristic emission energy of an element is slightly below the absorption edge energy. A pure element is therefore "transparent" to its own emission lines. Filter thicknesses were generally chosen to attenuate the X-ray beam by a factor of 2 to 5 at the wavelength of interest. Five anode targets (aluminum, carbon, copper, molybdenum and zirconium) were used for the VETA-I test. Their characteristic X-ray lines with mean line energy, operating anode voltages and corresponding filter thicknesses are listed in column 1 through 4 of Table 1.

3. X-RAY SOURCE SIZE MEASUREMENT

Understanding that the knowledge of the source size is crucial to the VETA test and the subsequent data analysis, a pinhole camera measurement of the source size was planned and carried out between June 18 and 20, at the XRCF. Figure 3 is a schematic diagram of the measurement setup. It is the same setup as shown in Figure 1, except instead of the Guide Tube a High Resolution Imager (HRI) is connected to the 6 inch gate valve and, instead of the filterwheel, a filter/pinhole holder is inserted near the X-ray Generator Head. The X-ray Generator Head is the actual one later used for the VETA test. The pinhole is a laser drilled 30 μm diameter circular hole on a 12.5 μm thick gold foil. The HRI is a microchannel plate detector with an area of 26.4 x 26.4 mm^2 and 25 μm FWHM resolution.[4] Its axis is tilted 2 degree from the X-ray pipe axis to increase the sensitivity. The distances are 170.7 mm between the source and the pinhole and 1500.9 mm between the pinhole and the HRI. This configuration gives a magnification factor 8.79. Therefore this pinhole camera has a 2.8 μm resolution for the source spots, which enables measuring the detailed spatial structures of the source. Keep in mind that 0.5 arcsec for VETA is 1.28 mm at the source. We will use this as a scale in the following figures and tables. Source spot from six anodes were measured with this pinhole camera. Table 1 lists representative measurements that have a good electron beam focus and source spot. From columns 5 to 10, there listed filters, anode voltage, emission current, integration time, HRI counts, and filename for each run. Please note that copper anode was not measured but later used for the VETA test, while magnesium and silicon anodes were measured but not used for VETA test. Because most of the

Table 1. X-ray Sources for the VETA and Pinhole Test

X-ray	Energy	VETA Test		Pinhole Test					
Line	keV	Filter μm	V kV	Filter μm	V kV	I mA	T sec	HRI cnts	File
Al-K	1.488	Al 10.0	8.0	None	8.00	0.18	30	7045	a_3_1
				None	8.01	0.106	90	13737	t20
				Al 25.4	8.06	2.01	45	6124	t23
C-K	0.277	Poly 2.0	4.0	None	2.10	0.17	300	9450	c_2_1
				None	5.03	0.40	30	6196	c_3_3
				Poly 12.7	5.02	2.01	30	6118	c_4_1
Cu-L	0.932	Cu 0.5	7.0						
Mo-L	2.334	Mo 2.0	17.0	None	7.00	0.50	15	4233	m_3_5
				None	8.00	0.10	60	5803	m_2_3
				Ag 2.0	9.02	0.50	20	4765	m_4_4
Zr-L	2.067	Zr 2.08	12.0	None	9.00	0.15	30	5507	z_3_2
				Ag 2.0	9.04	0.60	30	4809	z_4_2
				Ag 2.0	10.05	0.75	30	9113	z_4_3
Mg-K	1.254			None	6.00	0.50	30	7785	mg_3_1
				Al 25.4	8.02	4.01	30	3377	mg_4_1
Si-K	1.741			None	5.06	0.10	400	5497	s_2_2
				None	7.08	0.50	45	5763	s_3_2
				None	7.00	0.75	30	3993	s_4_3

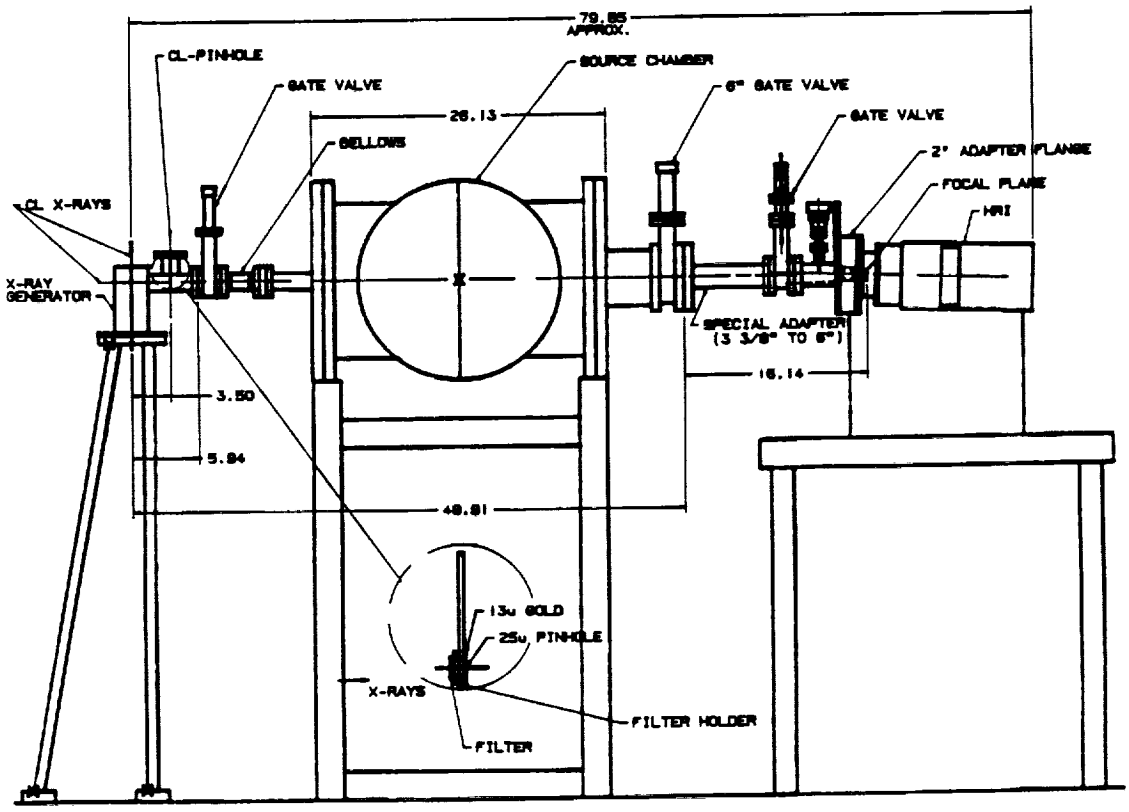

Figure 3: XRCF X-ray Source Size Measurement Setup.

VETA test X-ray filters were not available at that time, all of the low flux runs used no filters, and the high flux runs used filters not exactly matching the ones later used in the VETA test. This should not affect the source size because the filters were only used to suppress the continuum which is much weaker than the lines. The X-ray generator operating conditions (viz., emission current and bias voltage) were selected to be representative of those later used during the VETA-I test. The integration time was chosen to have at least 3000 HRI counts.

4. X-RAY SOURCE IMAGES AND DATA ANALYSIS

The recorded HRI data were stored on floppy diskettes and then transferred to our Sun Work Station. The data were analyzed and displayed with IRAF/PROS (Image Reduction and Analysis Facility / Post-Reduction Off-line Software) software system. We did deconvolution of the image by using Lucy's technique,[5] considering a tophat function as the Point Spread Function (PSF) of the 30 μm pinhole. Because the size of the pinhole PSF on the HRI (0.294 mm) is much smaller than that of the source image (see Figure 4), deconvolution of the image can hardly make any difference. Therefore we chose not to spend the time for image deconvolution. All the figures shown in this paper are from the original data.

Figure 4 shows one of the X-ray source images from an aluminum target. Figure 4(a) is a contour plot of the image with contour levels equal to 2, 10, 20, 35, 50, 65, 80, 90, 100 percent of the peak intensity. The X and Y axes are the horizontal and vertical directions of the source spot, respectively. Figure 4(b) is a 3D plot of the same image with 1 x 1 mm^2 area in the X-Y plane and intensity in the Z direction. The little circle in Figure 4(a) indicates the size of the 30 μm pinhole Point Spread Function on the HRI. It is much smaller than the source image size. Therefore the deconvolution process was not necessary. Figures 5 through 9 show the same kinds of plots for carbon, molybdenum, zirconium, magnesium, and silicon targets,

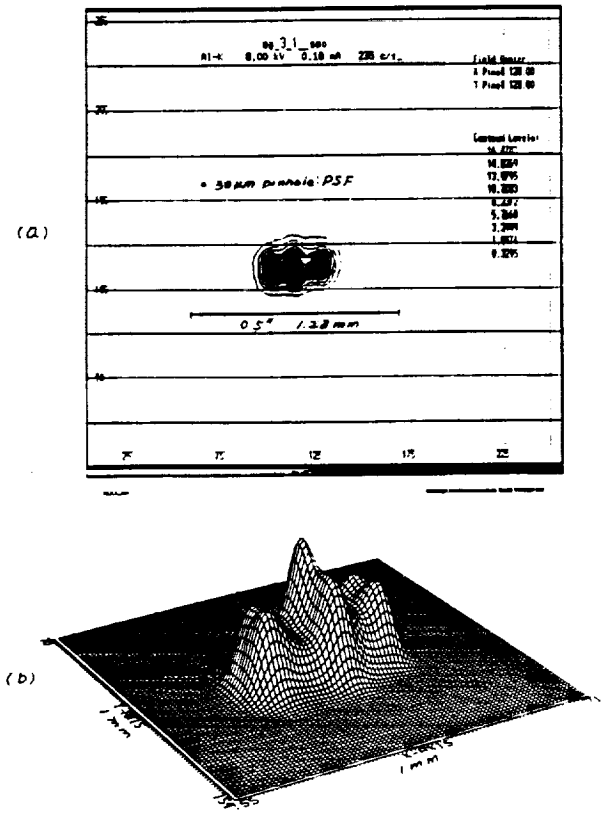

Figure 4: Aluminum Source Image.

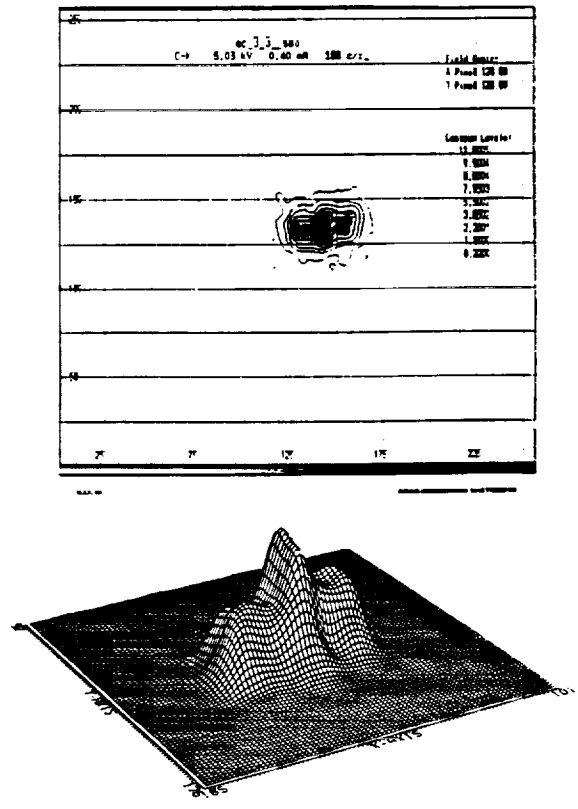

Figure 5: Carbon Source Image.

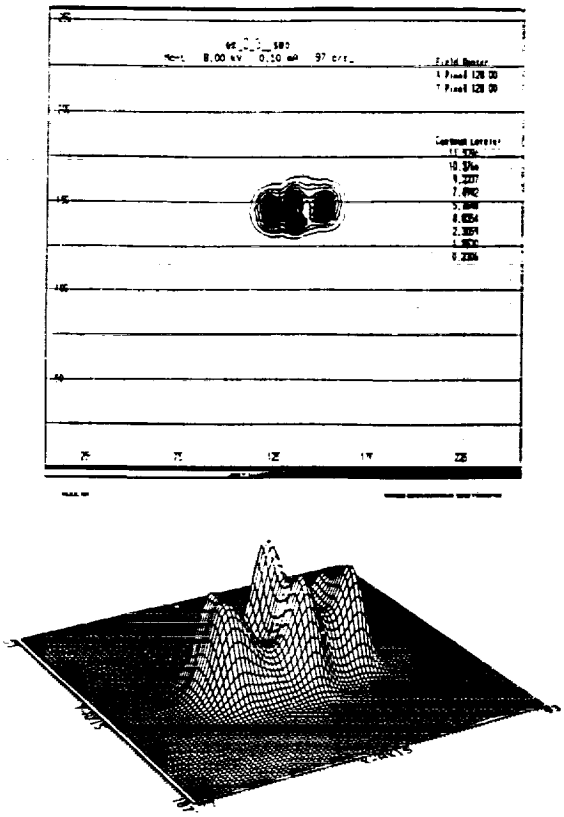

Figure 6: Molybdenum Source Image.

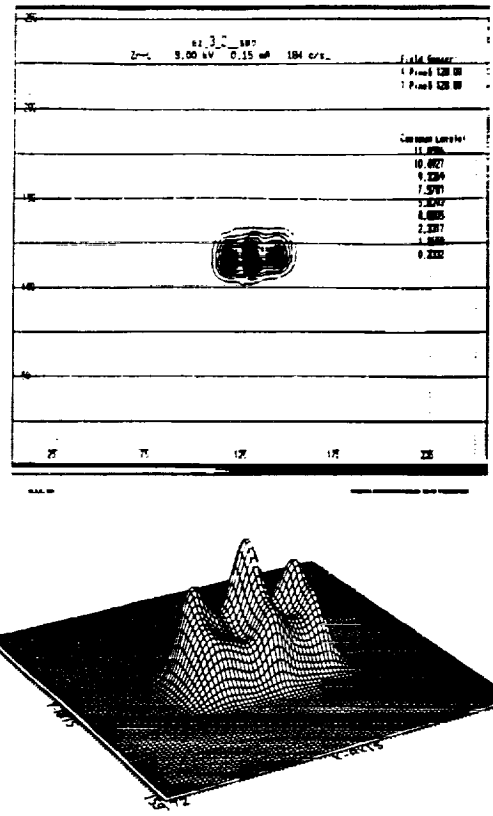

Figure 7: Zirconium Source Image.

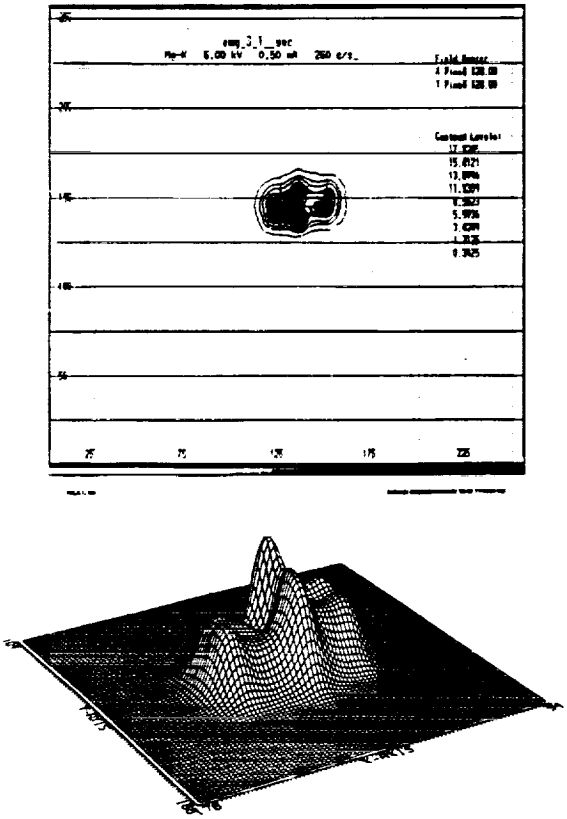

Figure 8: Magnesium Source Image.

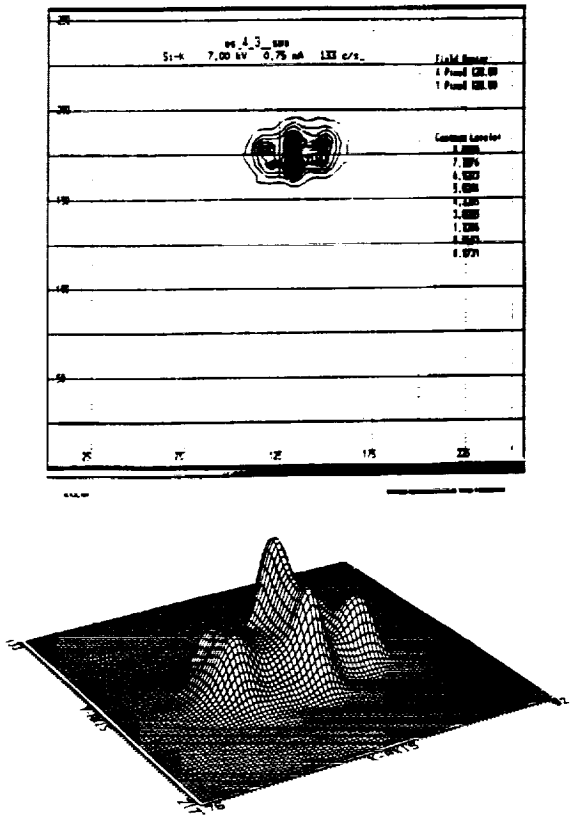

Figure 9: Silicon Source Image.

respectively. It is seen that all the images are about the same size and have similar structures. Generally speaking, the source spots are much smaller than 1.28 mm or 0.5 arcsec and a little narrower in the vertical direction (Facility Z-axis) than the horizontal direction (Facility Y-axis). A distinctive feature for all the images is that there are three intensity stripes along the vertical direction, which can also be seen in the anode pictures in the next section. This is probably due to the surface fine structure of the source filament. Figure 10 shows four microscope pictures of the filament, with magnification factors 35, 339, 1340 and 2820, respectively. There are many fine stripes along the filament. Because the electrons are most likely being

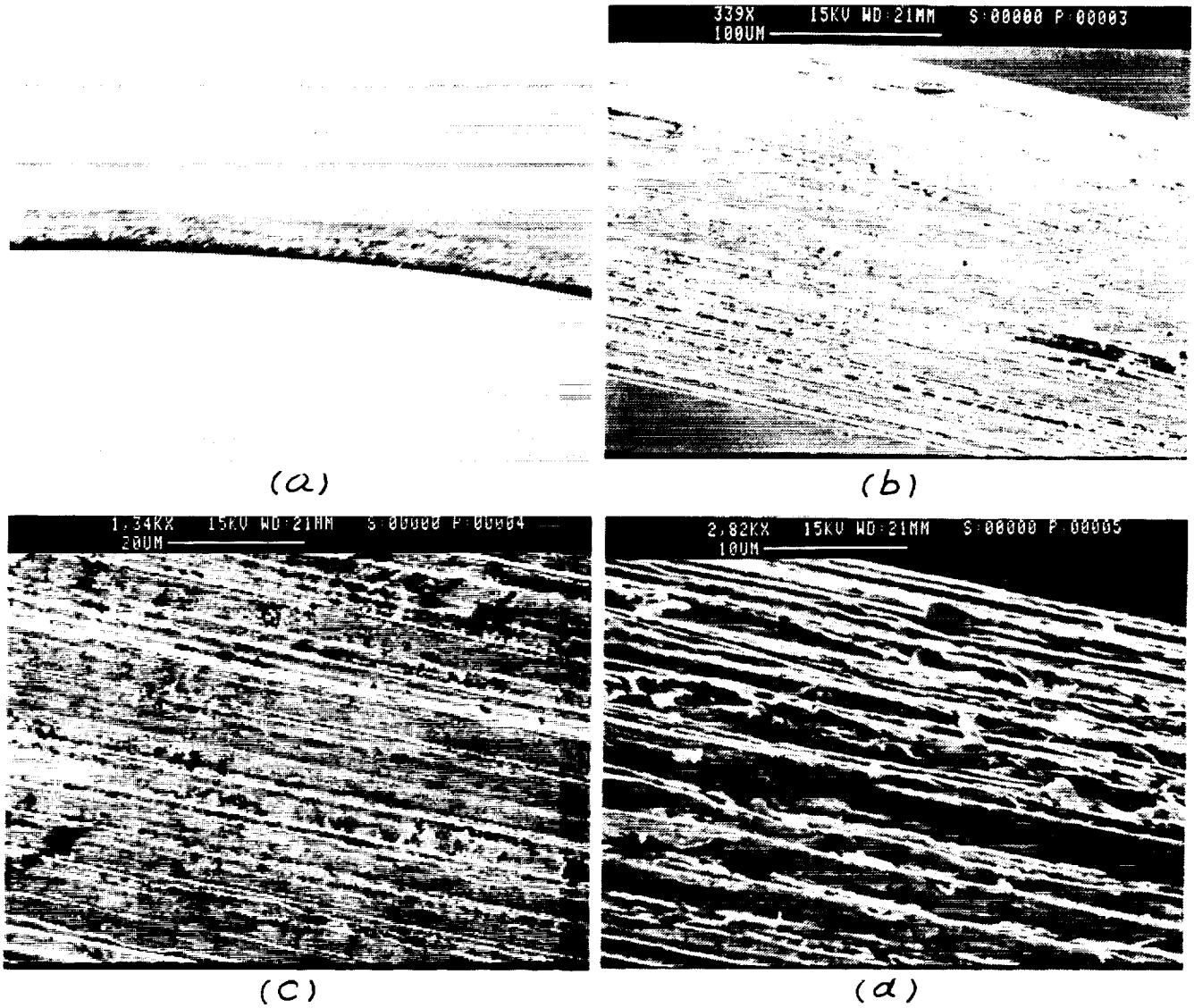

Figure 10: X-ray Source Filament Pictures. Magnification factors are (a) 35, (b) 339, (c) 1340 and (d) 2820. There are many fine stripes along the filament, which caused the three intensity peaks in the source.

emitted at the peak of the stripes and the filament is aligned in the X-ray direction, electron beams hit the anode target in this striped pattern. From the VETA point of view, the stripes are in the vertical direction, which agrees with the images recorded.

Figures 11 through 16 are the image profiles projected onto Y and Z axes. The image features mentioned above are clearly shown in these projection profiles. Since these are not Gaussian or any other type of regular profiles, we give six parameters to characterize the source size. They are the RMS, FWHM, and Full Width

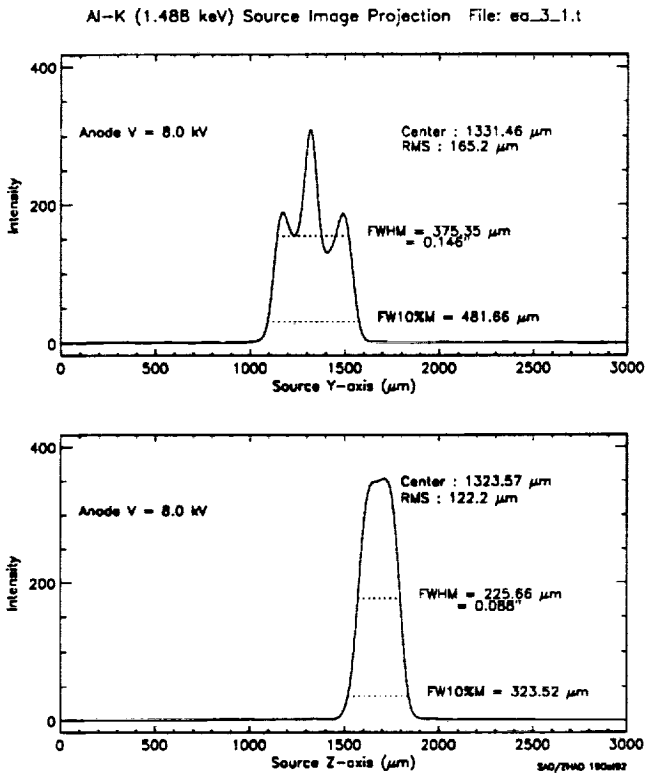

Figure 11: Aluminum Source Image Projection Profile.

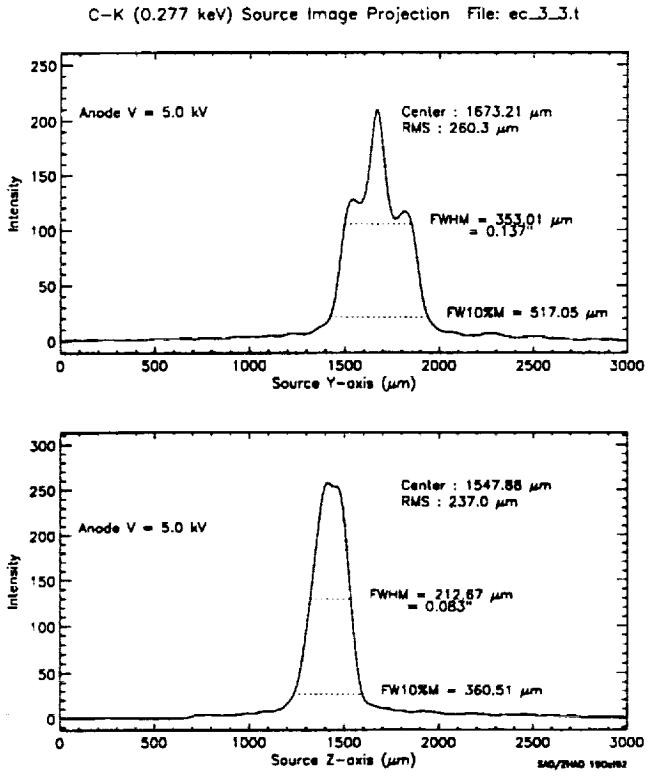

Figure 12: Carbon Source Image Projection Profile.

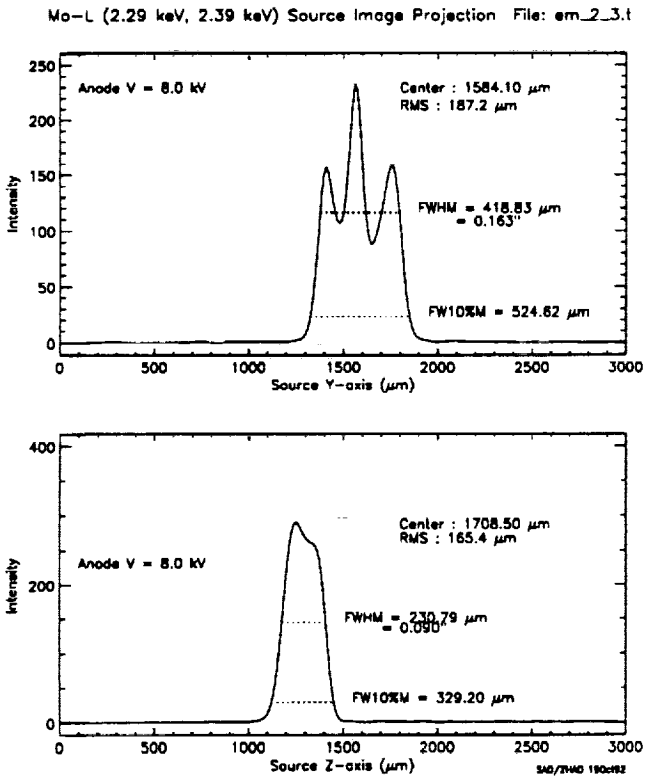

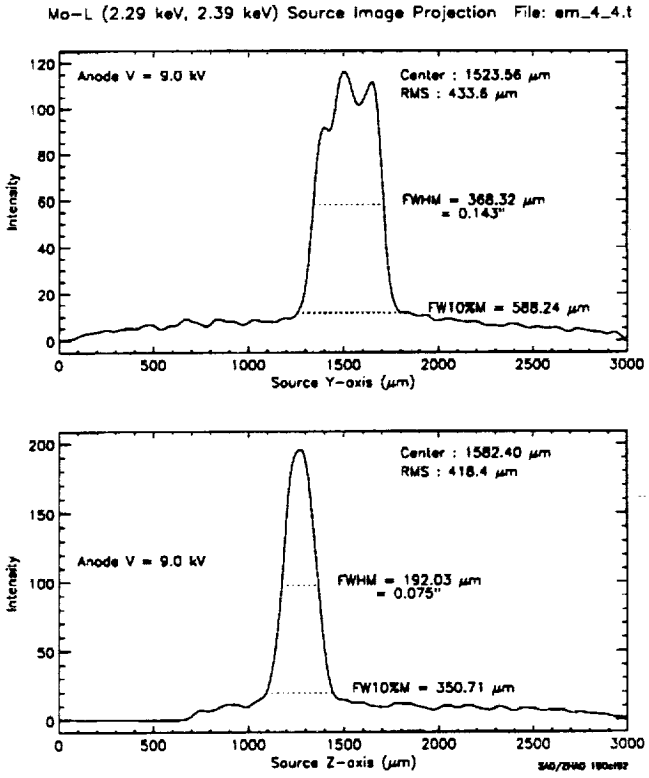

Figure 13: Molybdenum Source Image Projection Profile.

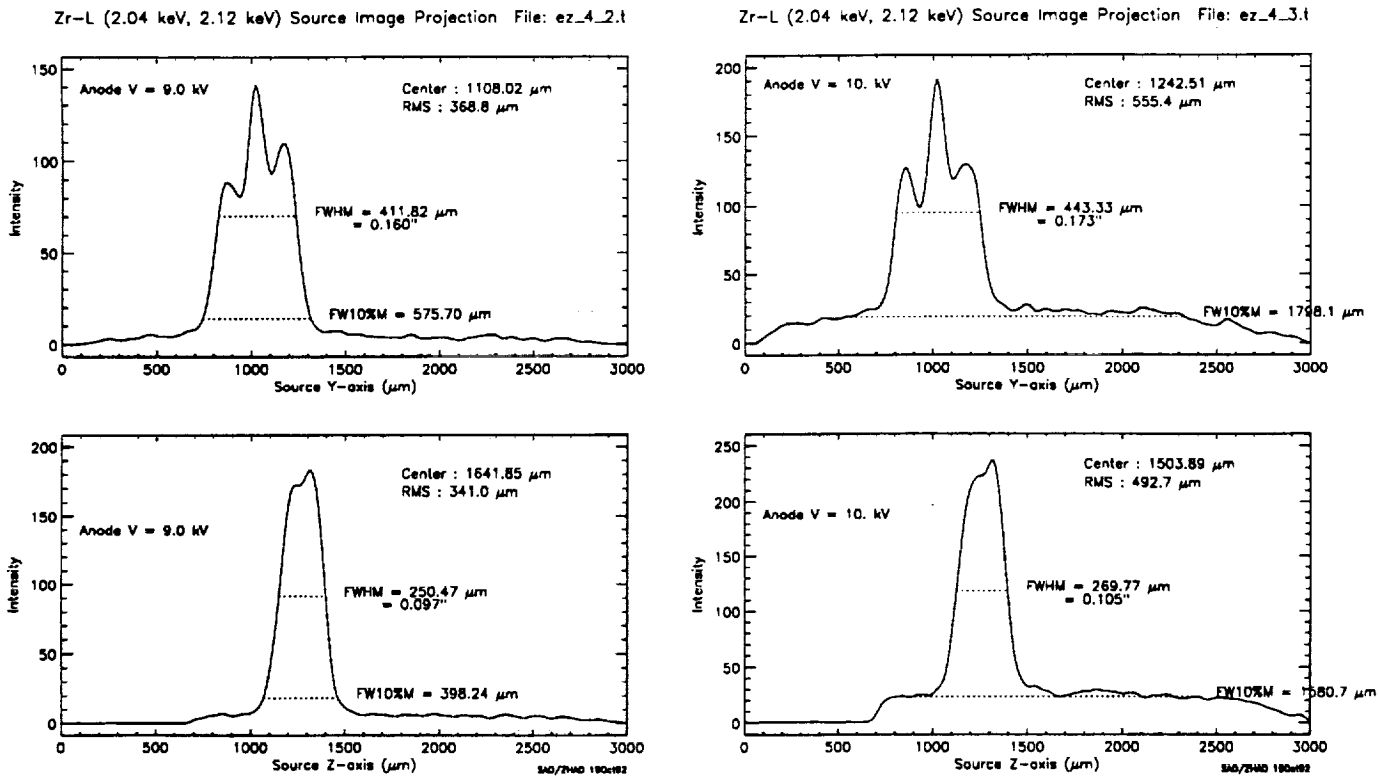

Figure 14: Zirconium Source Image Projection Profile.

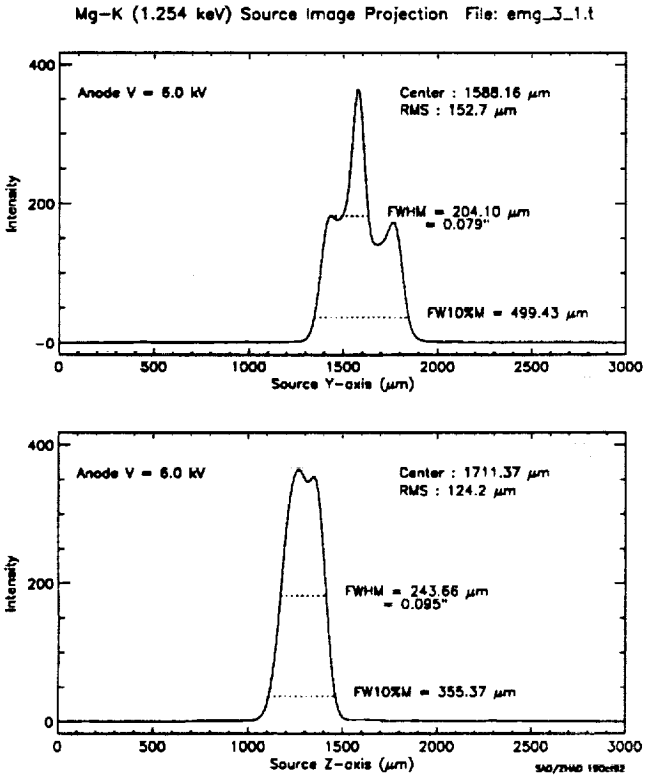

Figure 15: Magnesium Source Image Projection Profile.

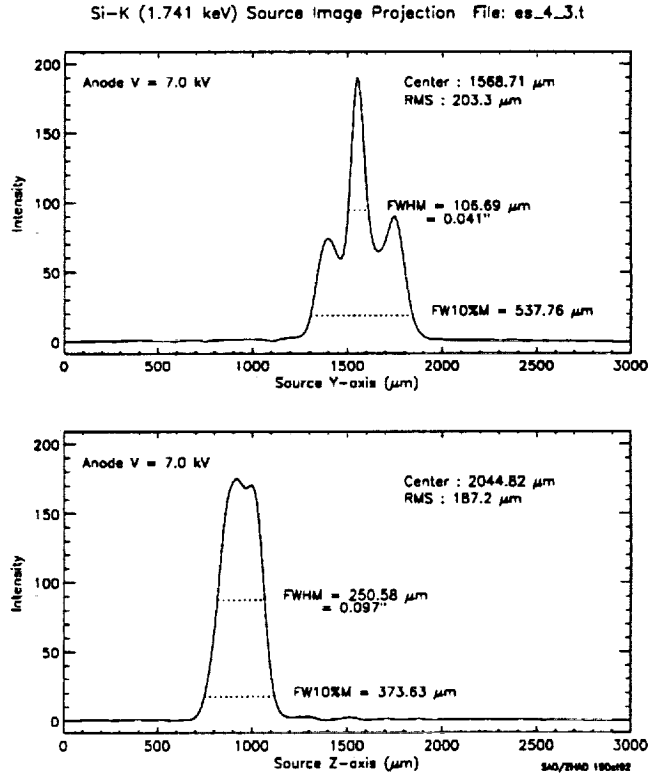

Figure 16: Silicon Source Image Projection Profile.

10% Maximum (FW10%M) in Y and Z directions. For all the images, the FWHM is less than 0.45 mm or 0.35 mm in horizontal or vertical directions, respectively. For aluminum and carbon targets, the pinhole test results here give the actual source intensity distribution for the VETA test since the operating conditions are the same for both tests. For molybdenum and zirconium targets, the anode voltage was set higher during the VETA test in order to achieve desired beam flux. Especially for molybdenum, the anode voltage for VETA test is 17 kV but the highest voltage used for the pinhole test is only 9 kV. This is mainly because the source molybdenum filter used for the VETA test was labeled incorrectly. A two micron molybdenum filter was requested but the actual thickness of the filter was 5.25 micron, found in the spectrum analysis after the VETA test.[3] This difference reduced the Mo-L line beam flux by a factor of 9. Without knowing that the thicker filter was used during the VETA test, the anode voltage was increased to obtain an adequate flux level. Therefore the pinhole test results do not reflect the real intensity distribution of the molybdenum and zirconium source during the VETA test. However, we still can use the pinhole test results to make an estimate. As we can see in Figure 13 and 14, a certain amount of halo appears around the source intensity peak when the anode voltage is increased, but the peak width and shape stayed about the same. We will show in the next section that this was true even for the VETA operating voltage.

5. X-RAY SOURCE ANODE PICTURES

During the VETA test, three microscope pictures, with magnification x7, x12.5 and x35, were taken for each used anode immediately after it was brought out from the X-ray Generator Head. Figure 17 shows the x7 and x35 pictures for the aluminum anode. Figures 18 through 21 shows the same pictures for the other four anodes used for the VETA test. These pictures were taken directly above the anode - a view angle 90 degrees from the VETA. The spots where electron beam hit the target and the X-rays were generated clearly match the source images taken by the pinhole camera, especially the three intensity stripes. The spot sizes from the pictures agree with the pinhole test results (Because the anode surface is 30 degrees from the horizontal, the source size in the vertical direction is the length of the spot in the picture divided by $\sqrt{3}$). However, the copper anode picture, which was not measured in the pinhole test, shows a different and bigger

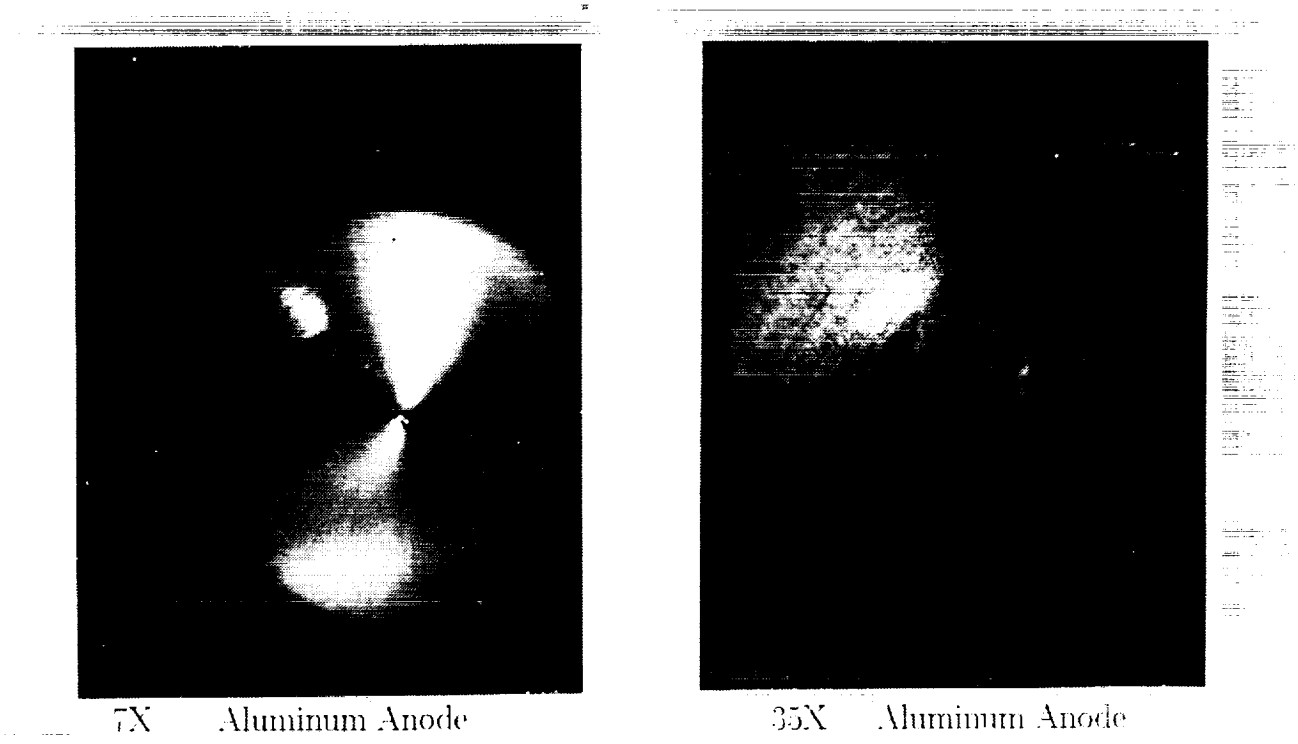

Figure 17: Aluminum Source Anode Pictures. ×7 (left), ×35 (right). Actual anode size: 10.7 mm diameter.

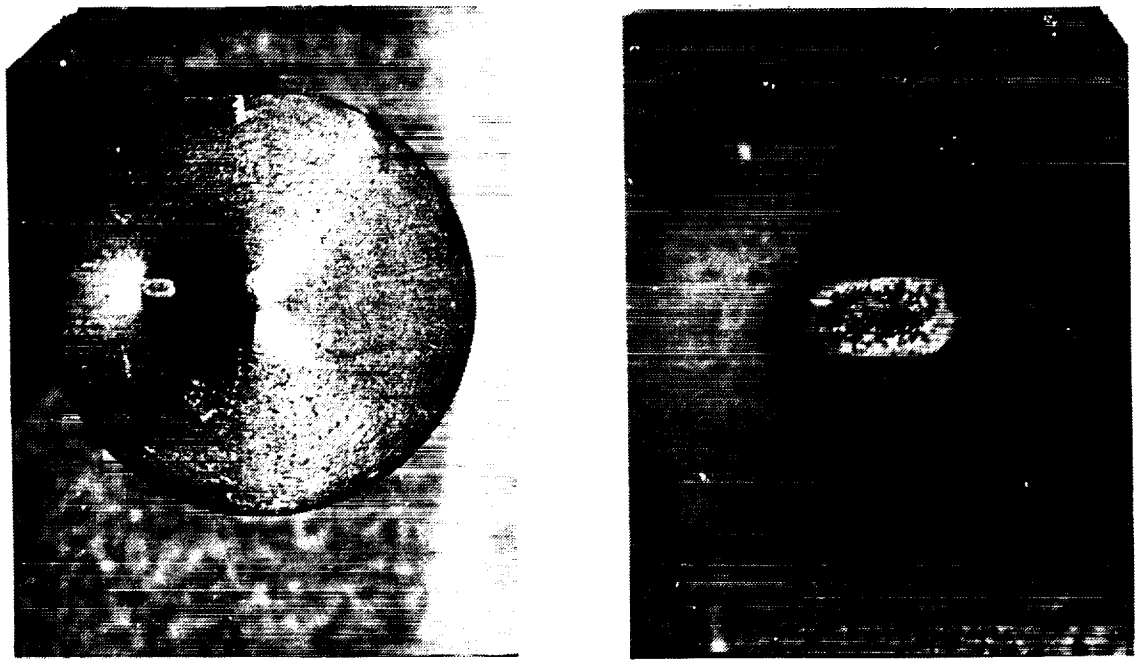

Figure 18: Carbon Source Anode Pictures. ×7 (left), ×35 (right). Actual anode size: 10.7 mm diameter.

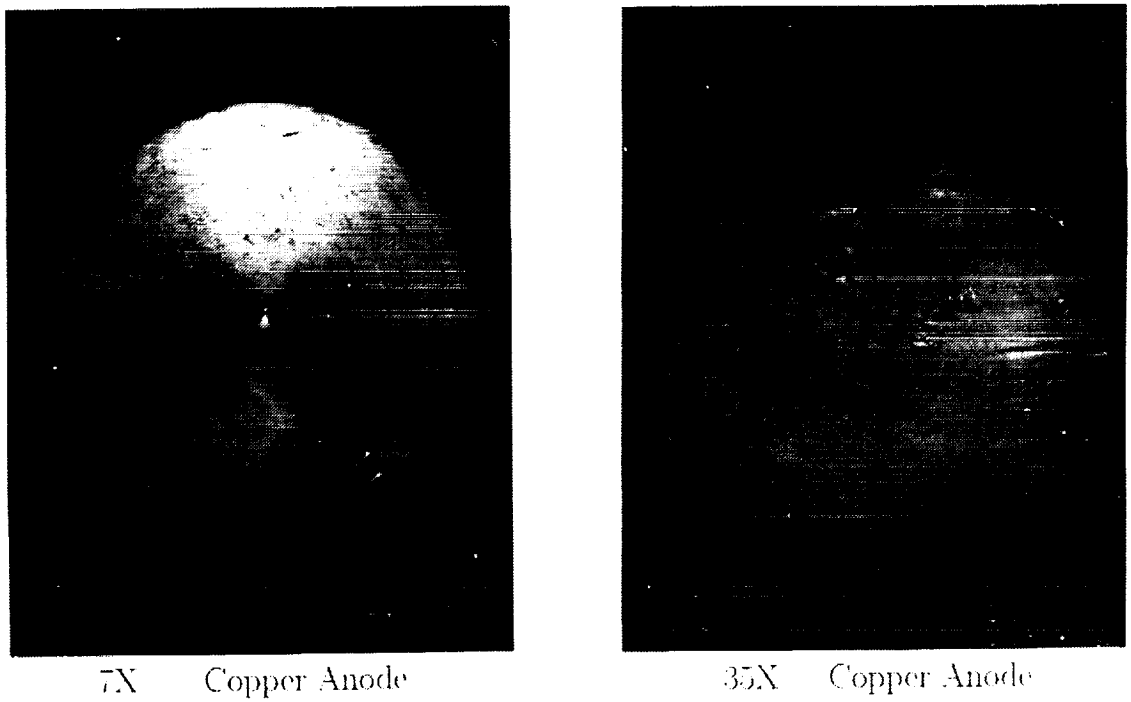

Figure 19: Copper Source Anode Pictures. ×7 (left), ×35 (right). Actual anode size: 10.7 mm diameter.

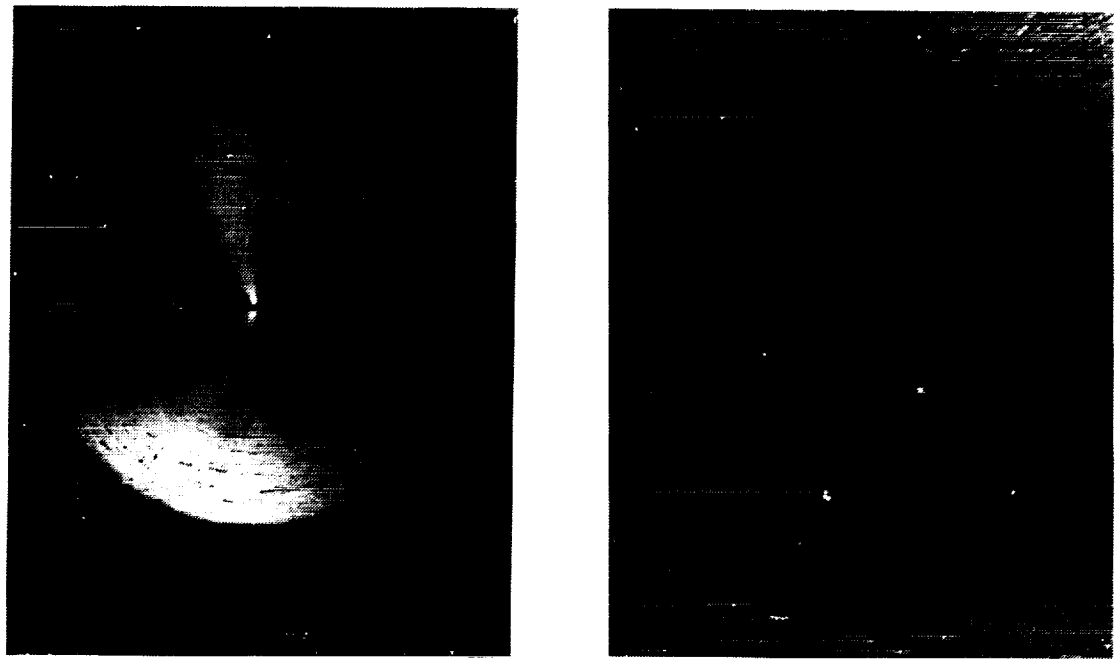

Figure 20: Molybdenum Source Anode Pictures. ×7 (left), ×35 (right). Actual anode size: 10.7 mm diameter.

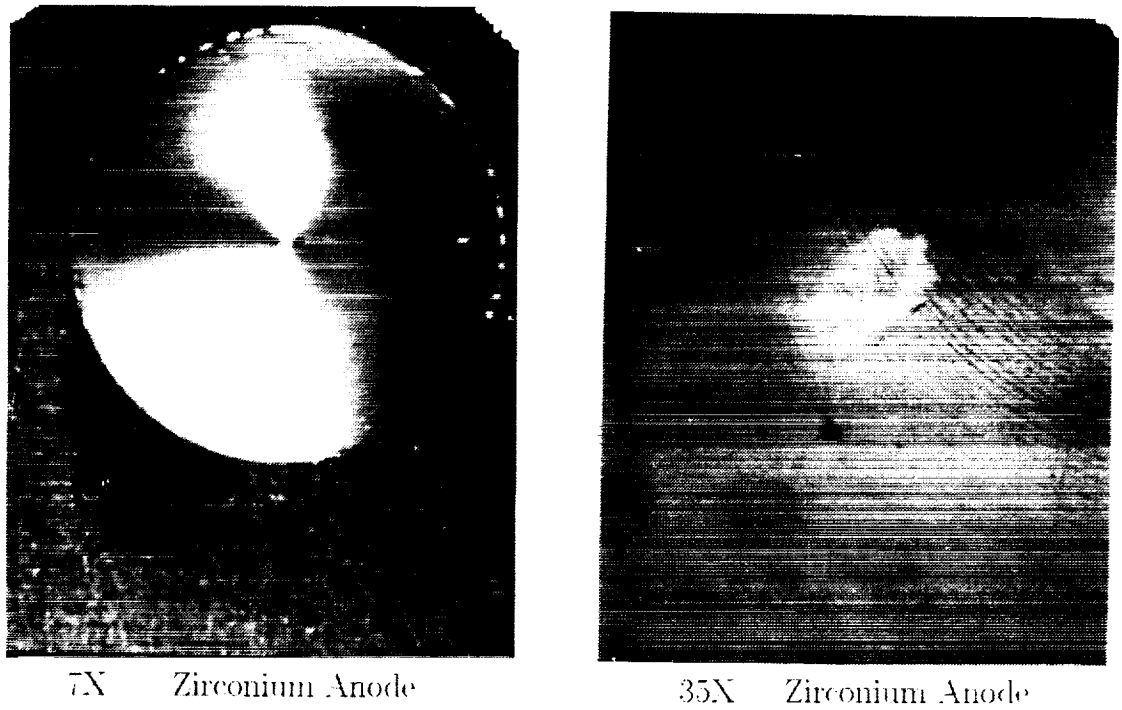

Figure 21: Zirconium Source Anode Pictures. ×7 (left), ×35 (right). Actual anode size: 10.7 mm diameter.

Table 2. X-ray Source Intensity Distribution Measurement Results

X-ray Line	Energy keV	Anode V kV	Width in	RMS		FWHM		FW10%M	
				mm	arcsec	mm	arcsec	mm	arcsec
Al-K	1.488	8.0	Y	.165	0.065	.375	0.147	.481	0.188
			Z	.122	0.048	.225	0.088	.323	0.126
C-K	0.277	5.0	Y	.260	0.102	.353	0.138	.517	0.202
			Z	.237	0.093	.212	0.083	.360	0.141
Cu-L[a]	0.932	7.0	Y	.23	0.09	.52	0.20	.66	0.26
			Z	.14	0.06	.25	0.10	.36	0.14
Mo-L	2.334	9.0[b]	Y	.433	0.169	.368	0.144	.588	0.230
			Z	.418	0.163	.192	0.075	.350	0.137
Zr-L	2.067	10.0[b]	Y	.555	0.217	.443	0.173	.1798	0.702
			Z	.492	0.192	.269	0.105	.1580	0.618
Mg-K	1.254	6.0	Y	.152	0.060	.204	0.080	.499	0.195
			Z	.124	0.049	.243	0.095	.355	0.139
Si-K	1.741	7.0	Y	.198	0.077	.397	0.155	.515	0.201
			Z	.177	0.069	.234	0.091	.342	0.134

[a] Width estimated from anode photo.
[b] Below the VETA operating voltage.

spot. We only made a rough estimate of its size based on our understanding of other anode pictures.

6. RESULTS AND DISCUSSIONS

Table 2 lists the final results of the X-ray source intensity distribution measurements. For each source size, it lists RMS, FWHM and FW10%M in both horizontal (Y) and vertical (Z) directions. For all the targets, the source sizes were smaller than the measured VETA FWHM. For the aluminum and carbon sources, of which we used to measure the FWHM of the VETA, the measurements were done under the same operating conditions as the VETA test. For molybdenum and zirconium sources, the measurements were done at a lower anode voltage than the VETA test. Combining the results of the pinhole test and the anode pictures, we conclude these two source sizes should still be the same even though there are more halos around the peaks. The copper source, of which we didn't make pinhole measurement, has a bigger size based on the anode picture. An accurate measurement of the VETA encircled energy and effective area was made only with the aluminum, carbon and zirconium sources.[6,7] The results of this X-ray source measurement were used to analyze the VETA data, to deconvolve the point spread function, to characterize the mirror surface figure and to predict its in orbit performances.[8,9]

7. ACKNOWLEDGEMENTS

We would like to thank Adrian Roy and Martin Zombeck for the pinhole camera testing and data taking. We also thank David Watson for operating the source and providing useful information about the XRCF X-ray Generator. This work was supported under NASA contract # NAS8-36123.

8. REFERENCES

1. M. C. Weisskopf, "The Advanced Astrophysics Facility: An Overview," *Astrophysical Letters & Communications*, Vol. 26, pp. 1-6, 1987.

2. E. M. Kellogg, R. J. V. Brissenden, K. A. Flanagan, M. D. Freeman, J. P. Hughes, M. T. Jones,

M. Ljungberg, P. Mckinnon, W. A. Podgorski, D. A. Schwartz, and M. V. Zombeck, "Calibration of the Verification Engineering Test Article-I (VETA-I) for AXAF using the VETA-I X-ray Detection System," *Proc. SPIE,* Vol. 1546, pp. 2-12, 1991.

3. G. Chartas, K. A. Flanagan, J. P. Hughes, E. M. Kellogg, D. Nguyen, M. V. Zombeck, M. Joy, and J. J. Kolodziejczak, "Correcting X-ray spectra obtained from the AXAF VETA-I mirror calibration for pileup, continuum, background and deadtime," *Proc. SPIE,* this volume, 1992.

4. W. A. Podgorski, K. A. Flanagan, M. D. Freeman, R. G. Goddard, E. M. Kellogg, T. J. Norton, J. P. Ouellette, A. G. Roy, and D. A. Schwartz, "VETA-I X-ray detection system," *Proc. SPIE,* this volume, 1992.

5. L.B. Lucy, "An iterative technique for the rectification of observed distributions," *Astronomical Journal,* Vol. 79, pp. 745-754, 1974.

6. P. Zhao, M. D. Freeman, J. P. Hughes, E. M. Kellogg, D. Nguyen, M. Joy, and J. J. Kolodziejczak, "AXAF VETA-I mirror encircled energy measurements and data reduction," *Proc. SPIE,* this volume, 1992.

7. E. M. Kellogg, G. Chartas, D. Graessle, J. P. Hughes, L. Van Speybroeck, P. Zhao, M. C. Weisskopf, R. F. Elsner, and S. L. O'Dell, "The X-ray reflectivity of the AXAF VETA-I optics," *Proc. SPIE,* this volume, 1992.

8. J. P. Hughes, D. A. Schwartz, A. Szentgyorgyi, L. Van Speybroeck, and P. Zhao, "Surface finish Quality of the Outer AXAF mirror pair based on X-ray measurement of the VETA-I," *Proc. SPIE,* this volume, 1992.

9. M. D. Freeman, J. P. Hughes, L. Van Speybroeck, J. W. Bilbro, M. C. Weisskopf, "Image analysis of the AXAF VETA-I mirror," *Proc. SPIE,* this volume, 1992.